Cancer Chemother Pharmacol (1997) 40: 495–505

ORGINAL ARTICLE

Laurence M. Levasseur · William R. Greco
Youcef M. Rustum · Harry K. Slocum

Combined action of paclitaxel and cisplatin against wildtype and resistant human ovarian carcinoma cells

Received: 24 October 1996 / Accepted: 5 March 1997

Abstract *Purpose*: The combination of paclitaxel (PTX) and cisplatin (DDP) shows good clinical efficacy against ovarian cancer. In order to examine the potential cellular basis for this, and provide leads as to how to optimize the combination, we examined the role of sequence of exposure to PTX and DDP on cell growth in vitro. *Methods*: Four human ovarian carcinoma cell lines, A121, A2780/WT, A2780/DX5B and A2780/CP3, two human head and neck carcinoma cell lines, A253 and FaDu, and the human ileocecal carcinoma cell line, HCT-8, were treated with PTX + DDP with seven schedules: (A) 96 h exposure to PTX + DDP; (B) 24 h PTX alone, then 72 h PTX + DDP; (C) 4 h DDP alone, then 92 h PTX + DDP; (D) 24 h PTX alone, 4 h DDP alone, then 68 h drug-free; (E) 4 h DDP alone, 24 h PTX alone, then 68 h drug-free; (F) 3 h PTX alone, 1 h DDP alone, then 92 h drug-free; and (G) 1 h DDP alone, 3 h PTX alone, then 92 h drug-free. Each of 66 two-drug experiments included five plates (440 randomly treated wells per experiment). Cell growth was measured by the sulforhodamine B assay. The nature and the intensity of the drug interactions were assessed by fitting a seven-parameter model to data with weighted nonlinear regression, enabling the estimation of an interaction parameter, α, with its standard error. *Results*: Overall there was very little departure from Loewe additivity: 43 experiments showed Loewe additivity, 10 showed Loewe antagonism, and 13 showed slight Loewe synergy. In vitro Loewe synergy was rare, was small when present, and reproducible only for the A121 and HCT-8 cells exposed to schedule D (24 h PTX prior to 4 h DDP). Isobolographic analysis showed complex combined-action surfaces with regions of local Loewe synergy and antagonism. *Conclusion*: It appears unlikely that the good clinical efficacy of the combination is primarily caused by a synergistic interaction at the cellular level.

Key words Taxol · Surface modeling · Isobol

Supported by RR10742, CA13038, CA65761 and CA16056

L.M. Levasseur · W.R. Greco (✉)
Department of Biomathematics, Roswell Park Cancer Institute, Buffalo, NY 14263, USA
Tel. 716-845-8641; Fax 716-845-8467

L.M. Levasseur · W.R. Greco · Y.M. Rustum · H.K. Slocum
Department of Experimental Therapeutics, Roswell Park Cancer Institute, Buffalo, NY 14263, USA

Introduction

Until the development of the taxanes, platinum-based therapy was considered to be the most active in the treatment of patients with ovarian cancer. Paclitaxel (Taxol, PTX), isolated from the Pacific yew, *Taxus brevifolia*, has demonstrated effectiveness against advanced and refractory carcinoma [37, 43]. Based upon the interesting clinical activities of the individual agents and a nonoverlapping spectrum of toxicity, cisplatin (cis-diamminedichloroplatinum (II), DDP) and PTX have been used together in several clinical trials. These trials addressed the therapeutic benefit of the combination in ovarian [29], lung [21], breast [18], head and neck [7], cervical [43] and gastrointestinal [1] carcinomas. Based on higher response rates, longer time to progression and marked improvement in median survival, the Gynecologic Oncology Group currently considers PTX + DDP as the new standard regimen for patients with advanced ovarian cancer [29]. Several factors may account for the therapeutic synergy such as (a) selective action of the combination against the malignant target relative to normal tissue toxicity, and (b) the large coverage of a heterogeneous tumor cell population and avoidance of cross-resistance as a result of the two agents having different mechanisms of action.

In vitro synergy has been reported for exposure to PTX prior to DDP, whereas the reverse sequence results in antagonism [20, 31, 39, 45]. There is no clear evidence for an intracellular origin of the schedule-dependent interaction, but several hypotheses have been proposed. Since exposure to DDP creates platinum–DNA

crosslinks, cells exhibit a phase G_2 block which might antagonize the antimicrotubule effect of PTX [27]. DDP could also interfere with the tubulin or the tubulin-associated proteins, therefore altering the tubulin binding site for PTX [32]. Finally, in vitro synergy might arise from a PTX-induced inhibition of the repair of DDP-DNA adducts [31, 34].

This paper reports the growth-inhibitory effects of the combination PTX + DDP performed on various drug-sensitive and -resistant human carcinoma cell lines continuously or sequentially exposed to the two drugs in combination. Through a rigorous qualitative and quantitative characterization of the two-drug interaction, the following questions were addressed. Is synergy at the cellular level possibly a major contributor to the clinical efficacy of PTX and DDP? What are the shapes of the in vitro combined-action response surfaces for PTX and DDP for a set of human cell lines and drug exposure schedules? Does drug resistance modify the in vitro interaction between PTX and DDP. Finally, does drug scheduling modulate the cellular response to the combination?

Materials and methods

Chemicals

RPMI-1640 cell culture medium, phosphate-buffered saline (PBS) and trypsin (0.05% in 0.53 m*M* ethylenediaminetetraacetic acid, tetrasodium salt) were obtained from Gibco (Grand Island, N.Y.), fetal calf serum (FCS) from Atlanta Biologicals (Norcross, G.) and DDP from Sigma Chemical (St. Louis, M.). PTX was provided by Bristol-Myers Squibb (Princeton, N.J.). Stock solution of PTX was made in methanol. DDP was dissolved in saline at 7.5 m*M*. The solubility of DDP was enhanced by warming the solution to 40 °C [16].

Cell lines

The human ovarian cell line A121 [4] was cultured in RPMI-1640 medium including 5% FCS. The subline A2780/CP3 was selected from the parental human ovarian carcinoma cell line A2780 [36] for resistance to DDP [28]. The A2780/DX5B was cloned from the doxorubicin-resistant subline, A2780/DX5 [19], and expressed the multidrug resistance (MDR) phenotype. Parental and resistant A2780 cells were grown in RPMI-1640 medium supplemented with 1% glutamine and 10% FCS. The human squamous carcinoma cells of the head and neck, A253 [11] and FaDu [33] were maintained in RPMI-1640 medium supplemented with 10% FCS. The human ileocecal adenocarcinoma cells HCT-8 were obtained from the American Type Culture Collection (Rockville, M.) and cultured in RPMI-1640 medium supplemented with 1 m*M* sodium pyruvate and 10% FCS. All the cell lines were maintained as monolayer cultures in 25-cm^2 flasks, incubated at 37 °C in a humidified atmosphere containing 5% CO_2. Cells were passed by trypsinization, twice weekly. Cell cultures were routinely tested bimonthly for mycoplasma, and found negative.

Growth inhibition assay

Exponentially growing cells were washed with PBS, trypsinized, counted and seeded at a density of 100 cells/well (6-day growth assay) or 200 cells/well (5-day growth assay) in 88 wells of 96-well microtiter plates and allowed to attach for either 24 h or 48 h. The eight remaining wells were filled with cell-free medium. Solutions of PTX and DDP in medium were freshly prepared from concentrated stock solution. Appropriate volumes were used to obtain drug mixtures at the five ratios 1:1, 2:1, 1:2, 4:1 and 1:4 of the drugs at their predicted IC_{50} values (e.g. a 1:1 ratio was prepared by mixing an equal volume of PTX at its predicted IC_{50} with DDP at its predicted IC_{50}). (In subsequent experiments the mixture ratios were calculated and are reported on an actual molar basis.) The agents alone and their mixtures were serially diluted over a 10^6-fold range of concentrations. Drug treatment of the cells was randomly assigned on the plates to minimize biases [25]. A typical experiment involved a stack of five 96-well plates with five replicates of each drug treatment condition (440 total data points and 40 blank wells).

Based on clinical reports [42], seven different schedules of exposure to the combination were investigated (Fig. 1). In schedule A, cells were simultaneously exposed to PTX and DDP for 96 h. In schedules B and C, cells were pretreated with PTX for 24 h, or DDP for 4 h, before the administration of the other agent. For schedules D, E, F and G, the exposure to PTX and DDP involved a drug-removal step at the end of each drug-exposure period. Cells were washed twice with RPMI-1640 medium, then exposed to drug-containing or drug-free medium. Cell growth inhibition was assessed on day 5 (A, B and C) or day 6 (D, E, F and G) by the sulforhodamine B assay [40]. Briefly, plates were fixed with 10% trichloracetic acid, washed with water and stained with sulforhodamine B. Unbound dye was removed with 1% acetic acid and protein-bound dye was extracted with Tris base. The optical density was read at 570 nm in a plate reader, and the data written to disk for importation to Excel (version 5.0. Microsoft), and analysis by the Universal Response Surface Approach [6, 8, 14, 15] described below.

Universal Response Surface Approach

By assuming the Hill model (Eq. 1) as the structural model for the concentration-effect curve of each agent alone and the Loewe

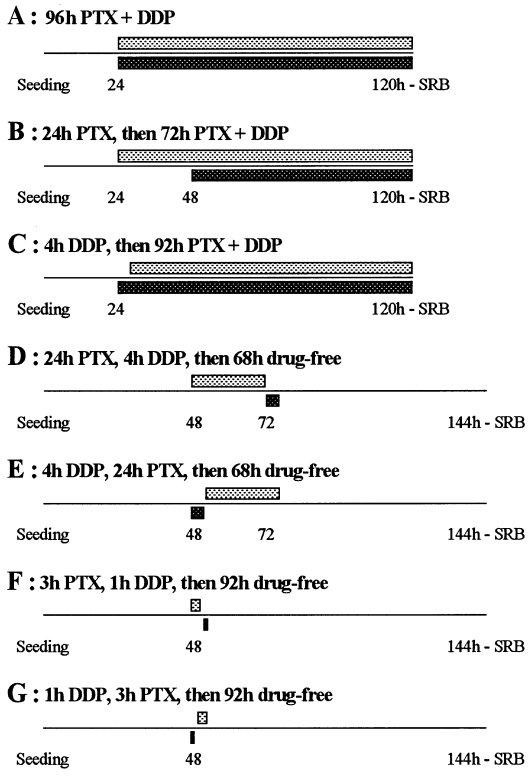

Fig. 1 Seven schedules of in vitro exposure to the combination PTX (▨) + DDP (■)

additivity model (Eq. 2), a Loewe synergism/Loewe antagonism model (Eq. 3) was derived [14]. (For an extensive discussion of rival nomenclature for drug combined action, see reference 15.) Equation 3 was fitted to the experimental data with iteratively reweighted nonlinear regression, enabling the estimation of an interaction parameter, α, along with its standard error. The magnitude of this parameter is directly related to the intensity of the interaction and to the degree of bowing of the isobol. When α is positive, Loewe synergy is indicated, whereas a negative value of α reflects Loewe antagonism. The interaction is Loewe additive if the 95% confidence interval for α encompasses zero. In Eq. 1, E is the measured effect, C is the concentration of drug, E_{con} is the control response, B is the background, IC_{50} is the concentration of drug inducing a 50% inhibition of the maximal cell growth and m is the slope parameter of the concentration-effect curve. Appropriate weights for fitting Eq. 3 to the raw data were obtained from modeling of the structure of the measurement error of the data with Eq. 4. The weighting factor used is the reciprocal of the predicted response raised to the power ϕ_3, where ϕ_3 is the slope of the log–log relationship between variance s_A^2 and mean $\overline{X}_A$ for a set of replicates [25]; a ϕ_3 slope equal to 2 would indicate a constant coefficient of variation.

$$E = B + \frac{(E_{con} - B)\left(\frac{C}{IC_{50}}\right)^{m}}{1 + \left(\frac{C}{IC_{50}}\right)^{m}} \quad \text{(Eq. 1)}$$

$$1 = \frac{C_1}{IC_{50,1}\left(\frac{E-B}{E_{con}-E}\right)^{\frac{1}{m_1}}} + \frac{C_2}{IC_{50,2}\left(\frac{E-B}{E_{con}-E}\right)^{\frac{1}{m_2}}} \quad \text{(Eq. 2)}$$

$$1 = \frac{C_1}{IC_{50,1}\left(\frac{E-B}{E_{con}-E}\right)^{\frac{1}{m_1}}} + \frac{C_2}{IC_{50,2}\left(\frac{E-B}{E_{con}-E}\right)^{\frac{1}{m_2}}} + \frac{\alpha C_1 C_2}{IC_{50,1}IC_{50,2}\left(\frac{E-B}{E_{con}-E}\right)^{\frac{1}{2m_1}+\frac{1}{2m_2}}} \quad \text{(Eq. 3)}$$

$$s_A^2 = \phi_2 \overline{X}_A^{\phi_3} \quad \text{(Eq. 4)}$$

Isobologram analysis

Individual fittings of the Hill model (Eq. 1) to experimental data were performed for each concentration-effect curve for the single agent alone and for each constant ratio mixture of PTX and DDP, with iteratively reweighted nonlinear regression. Adapted from the approach of Gessner [10], the IC_{50} values with accompanying 95% confidence intervals were plotted on a normalized isobologram. Plots were also made for the 10%, 25%, 75% and 90% effect levels.

Statistical software

The fitting of the nonlinear models to data was performed with software written in FORTRAN by our group [15]. All graphs were prepared with Sigmaplot (Jandel Scientific, San Rafael, Calif.). Software was run on Pentium-based microcomputers.

Results

In order to characterize the action of each agent alone, Eq. 1 was fitted to the growth inhibition data arising from single drug exposure from each of 98 separate experiments, and IC_{50} values (measure of potency) and slope parameters (measure of cellular heterogeneity in drug response) were estimated. The IC_{50} estimates of PTX and DDP for various periods of exposure are plotted in Figs. 2A and 3A, respectively. To facilitate comparison of the differences in potency between the agents, the same logarithmic scale was used for the *Y*-axes of the two figures. PTX appears to be a highly potent agent, active in the nanomolar range for long-term exposure, whereas the IC_{50} estimates for DDP are in the micromolar range. The A2780/DX5B ovarian line was resistant to PTX, as was expected owing to a high level of expression of the P-glycoprotein P-170. Relative to the A2780/WT cells, the degree of resistance to PTX

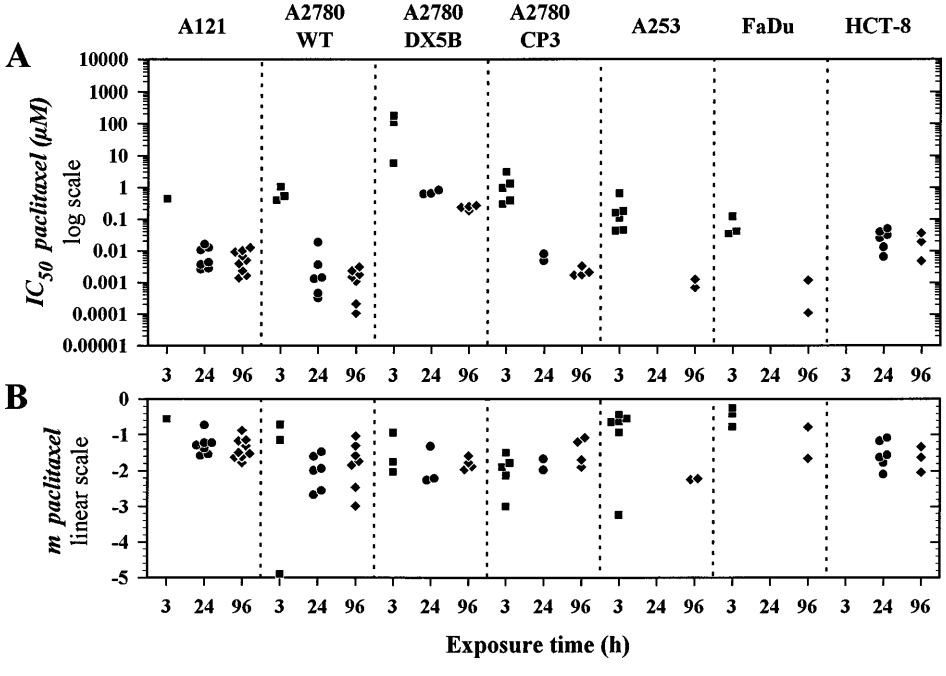

Fig. 2A,B Distribution of the IC_{50} values (**A**) and slopes m (**B**) for PTX as a function of the cell line and the duration of exposure to the agent. Each data point is the parameter estimate from a separate study

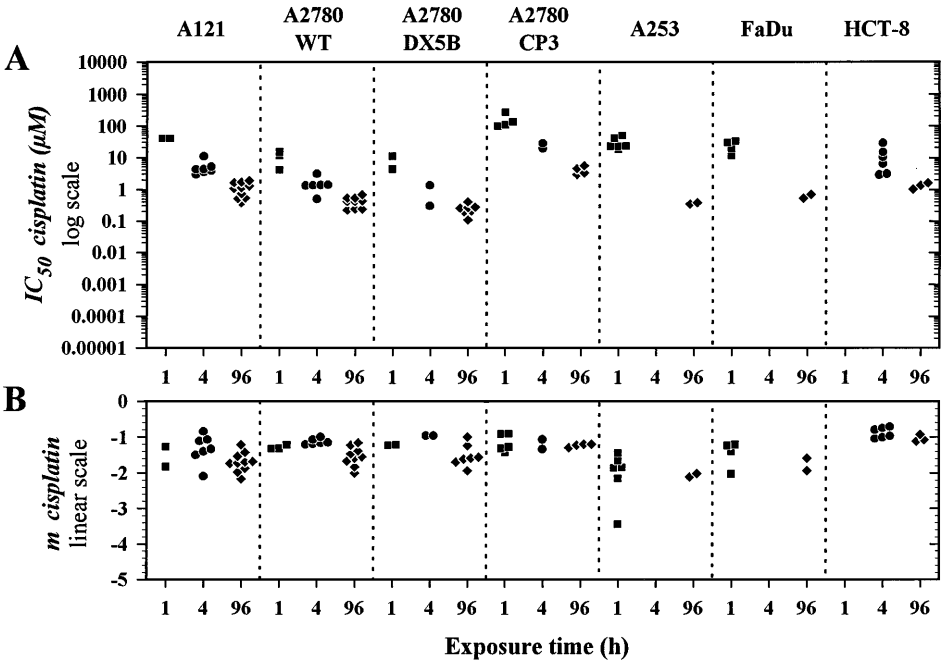

Fig. 3A,B Distribution of the IC_{50} values (**A**) and slopes m (**B**) for DDP as a function of the cell line and the duration of exposure to the agent. Each data point is the parameter estimate from a separate study

of the MDR derivative was about 150-fold. The HCT-8 colon cells were moderately resistant to PTX, with IC_{50} values increased by a factor of 6.5 and 14 for the 24 h and 96 h exposures, respectively. The head and neck lines, A253 and FaDu, were slightly more sensitive to PTX. Compared to A2780/WT, the potency of PTX for the 96 h exposure was increased by a factor of 2.3 in the FaDu cells and 1.5 in the A253 cells. DDP displayed similar potencies for the same exposure time among the various cell lines, except in the A2780/CP3. The resistance of A2780/CP3 is a consequence of a higher intracellular glutathione content, and an enhanced capacity for DNA damage repair [28]. This cell line exhibited an 18-, 16- and 10-fold degree of resistance for DDP for the 1 h, 3 h and 96 h exposures, respectively. No cross-resistance between PTX and DDP was noted.

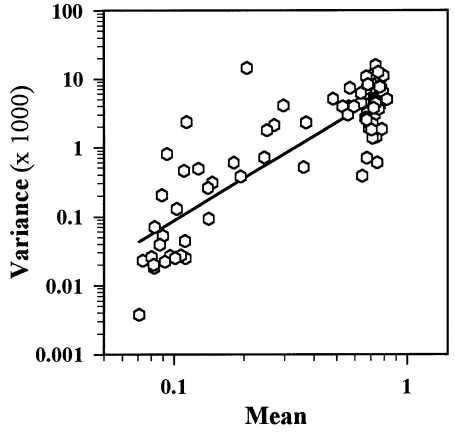

Fig. 4 Variance plot on log coordinates. Each symbol is the average of a set of five replicates and is plotted against the associated variance. The line was fitted to the log-transformed data with unweighted linear regression

Figures 2B and 3B display the estimated slope parameters m for PTX and DDP, respectively. The same linear scale was used for the two figures. PTX tended to induce a steeper cell growth inhibition curve (higher absolute values of the estimate of m) as the duration of exposure increased. This implies less heterogeneity of drug effect at longer exposure times. In contrast, the slope parameter estimates of the DDP-mediated growth inhibition curves were similar for exposure times ranging between 1 h and 96 h.

In order to assess the nature and the intensity of drug interaction, Eq. 3 was fitted to the data from each PTX + DDP experiment with iteratively reweighted nonlinear regression. Figures 4–7 illustrate our general data analysis approach for one representative experiment: the growth inhibition of the A2780/CP3 cell line exposed to the combination with schedule D. In Fig. 4, the variance for each of 88 sets of five replicates is plotted against the mean on log–log scales. A simple straight line was fitted to the log-transformed data with unweighted linear regression. The slope equal to 2.03 corresponds to the ϕ_3 parameter of Eq. 4. For fitting Eq. 3, raw data were weighted by the reciprocal of the predicted effect raised to the power 2.03. Figure 5 presents the three-dimensional concentration-effect surface fitted to the entire set of data (440 data points). For better visualization, the raw data were averaged among replicates, divided by the control response (E_{con} estimate) and expressed as the percentage of inhibition of cell growth. The fishnet surface was simulated from Eq. 3 with the best fitting parameters: $E_{con} = 0.742$, $IC_{50,\ PTX} = 5.46$ nM, $m_{PTX} = -1.52$, $IC_{50,\ DDP} = 38.2$ μM, $m_{DDP} = -1.17$, $B = 0.0883$ and

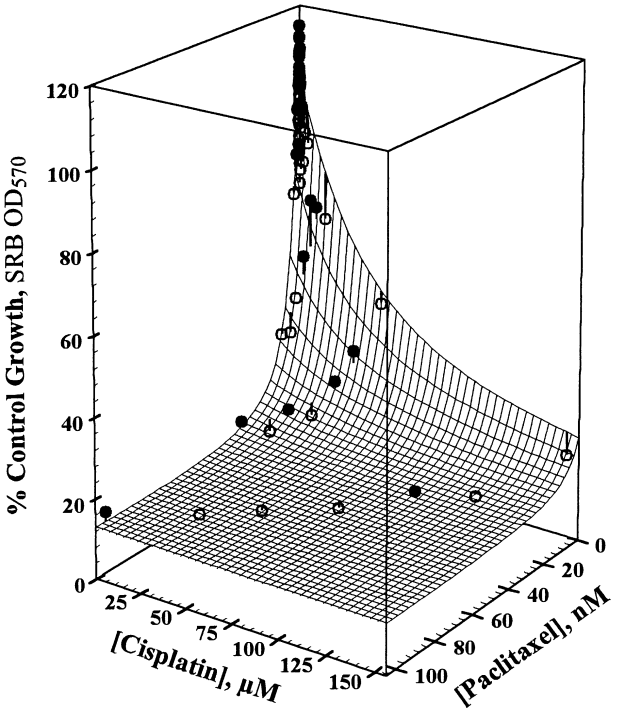

Fig. 5 Three-dimensional concentration-effect surface modeling of the combination PTX + DDP (schedule D) in A2780/CP3 cells. Symbols are the means of five replicates expressed as the percentage of the control response (E_{con} estimate). *Solid points* (●) are above the surface; *open points* (○) fall below the surface. *Vertical lines* connect each point to the surface. The predicted grid surface was simulated from Eq. 3 with parameters: $E_{con} = 0.742$, $IC_{50,\,PTX} = 5.46$ nM, $m_{PTX} = -1.52$, $IC_{50,\,DDP} = 38.2$ μM, $m_{DDP} = -1.17$, $B = 0.0883$ and $\alpha = 0.245$

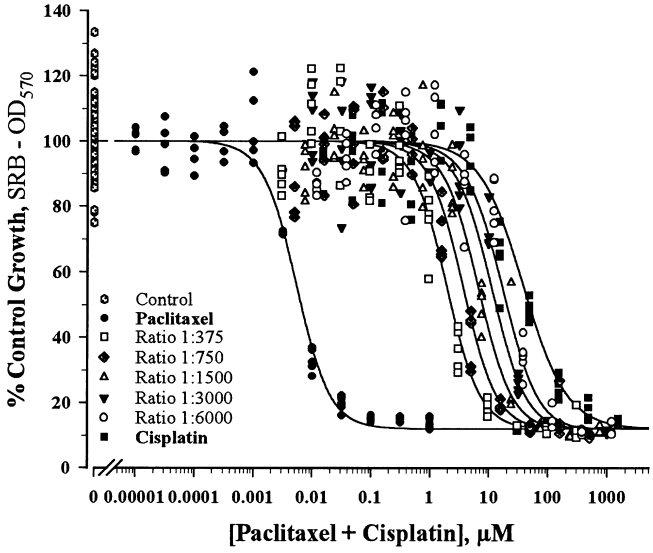

Fig. 6 Two-dimensional representation of the interaction surface displayed in Fig. 5. The cell growth inhibition induced by each constant ratio of PTX:DDP is plotted against the sum of PTX and DDP concentrations. Symbols are the experimental data points expressed as the percentage of the control response (E_{con} estimate). The curves are the vertical slices through the 3-D surface of Fig. 5 for the agents alone and for the constant ratios of PTX:DDP of 1:375, 1:750, 1:1500, 1:3000 and 1:6000

$\alpha = 0.245$. The 95% confidence interval for α was [−0.0474–0.538]. Since it encompassed zero, a Loewe additive interaction was concluded. Figures 6 and 7 are two-dimensional representations of the three-dimensional surface displayed in Fig. 5. For Fig. 6, the surface was cut along each fixed ratio of PTX:DDP and each of the seven vertical slices was plotted versus the sum of the concentrations of PTX and DDP (logarithmic concentration scale). For Fig. 7, horizontal slices were made in the surface at 10%, 50% and 90% inhibition of cell growth. The plots were normalized by division by the IC_X (X = 10, 50, 90) of PTX or DDP when given alone. The points are the estimated normalized IC_X values with accompanying 95% confidence intervals. The curves are the Loewe additivity reference line (straight diagonal line) and the isobol simulated for α equal to 0.245 (thick curved solid line). The dotted envelope is the 95% confidence interval around the estimated isobol.

Results from 66 PTX + DDP combination experiments are reported in Table 1. The estimate of the interaction parameter α is reported with its standard error. Overall, very few departures from Loewe additivity were observed; 10 experiments yielded Loewe antagonism, 43 yielded Loewe additivity, and 13 yielded slight Loewe

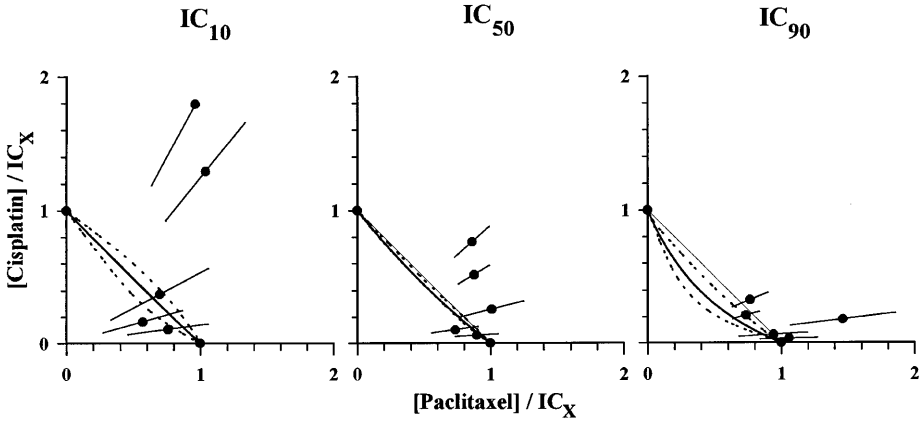

Fig. 7 Isobolographic plots at 10%, 50% and 90% inhibition of cell growth. The points are the observed IC_X values (X = 10, 50, 90) with accompanying 95% confidence intervals (line segments through the points). The curves include the theoretical Loewe additive isobol (*straight diagonal line*) and the simulated isobol for α equal to 0.245 (*thick curved solid line*) with its 95% confidence envelope (*dotted lines*)

Table 1 Qualitative and quantitative characterization of the interaction between PTX and DDP, via the Universal Response Surface Approach, in relation to the seven schedules investigated and the seven human cell lines exposed to the combination. The results are presented as qualification of the interaction, e.g. Loewe additivity (*ADD*), Loewe synergy (*SYN*) or Loewe antagonism (*ANT*), followed by the estimate ± standard error of the interaction parameter α. Results from replicate experiments are shown in the same cell of the table

	A	B	C	D	E	F	G
A121	ADD −0.00514 ± 0.033 ADD −0.00348 ± 0.057 ADD 0.0141 ± 0.048	ADD 0.0179 ± 0.076	ADD 0.00899 ± 0.025	SYN 1.40 ± 0.23 SYN 0.643 ± 0.11 SYN 0.733 ± 0.12	ADD 0.0983 ± 0.051 ADD −0.0104 ± 0.027 ADD −0.00794 ± 0.0078	ADD 0.957 ± 0.57	SYN 0.706 ± 0.18
A2780 WT	ADD 0.00497 ± 0.035 ADD −0.00482 ± 0.045 ANT not quantified	ADD −0.0152 ± 0.054	ADD −0.0144 ± 0.037	ANT −0.390 ± 0.062 SYN 0.335 ± 0.11 ADD 0.0266 ± 0.069	ADD 0.0322 ± 0.050 ADD 0.0148 ± 0.032 ADD −0.0854 ± 0.054	ADD 1.56 ± 2.1 ADD 0.128 ± 0.065	ADD 0.164 ± 0.13
A2780 DX5B	ADD −0.0246 ± 0.015	SYN 0.134 ± 0.041	ADD −0.0238 ± 0.017	ADD 0.00783 ± 0.049	ADD 0.0101 ± 0.038	ANT −0.0448 ± 0.0046	ANT −0.131 ± 0.011
A2780 CP3	ANT −0.0157 ± 0.0010 ADD 0.00940 ± 0.074	ADD 0.0447 ± 0.10	ANT −0.0198 ± 0.0070	ADD 0.245 ± 0.15	ADD 0.0127 ± 0.040	SYN 0.711 ± 0.28 ADD 0.319 ± 0.22	SYN 2.00 ± 0.79 ADD −0.0751 ± 0.066 ADD 0.147 ± 0.13
A253	ANT −0.0273 ± 0.0056 ADD 0.0724 ± 0.050	–	–	–	–	SYN 0.697 ± 0.18 ADD 0.0223 ± 0.078	SYN 0.437 ± 0.16 ADD 0.00905 ± 0.039
FaDu	ADD 0.00395 ± 0.033 ADD −0.00285 ± 0.034	–	–	–	–	ADD −0.0257 ± 0.014 ADD 0.114 ± 0.067	ADD −0.00419 ± 0.0031 ADD 0.0179 ± 0.018
HCT-8	ANT −0.122 ± 0.0053 ANT −0.374 ± 0.050 ADD 0.00687 ± 0.080	–	–	SYN 0.526 ± 0.18 SYN 0.824 ± 0.14 SYN 0.571 ± 0.094	ANT −0.194 ± 0.041 ADD 0.00437 ± 0.013 ADD −0.00787 ± 0.0061	–	–

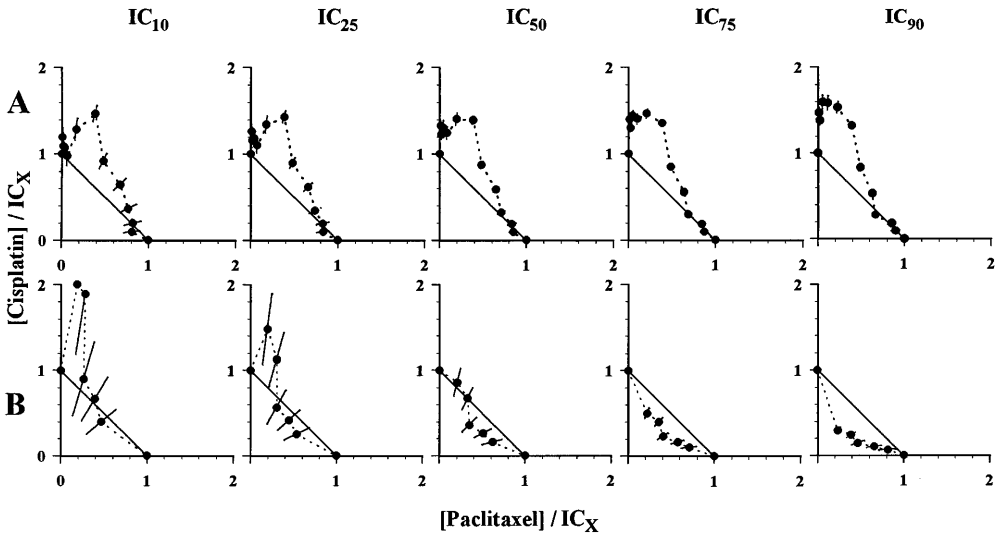

Fig. 8A,B Sets of normalized isobologram for 10%, 25%, 50%, 75% and 90% inhibition of cell growth: **A** a Loewe antagonistic interaction ($\alpha = -0.0273 \pm 0.0056$) for the A253 line treated with schedule C; **B** an example of Loewe synergy ($\alpha = 1.40 \pm 0.23$) for the A121 line treated with schedule D. The points are the observed C_X values (X = 10, 25, 50, 75, 90) with accompanying 95% confidence intervals. The *straight diagonal line* is the theoretical Loewe additivity line

synergy. Only 2 out of the 13 examples of significant Loewe synergy had an α estimate greater than 1. In general, the occasional observations of Loewe antagonism or Loewe synergy were not confirmed with repeat experiments. The two exceptions to this generalization were the cases of A121 cells exposed to schedule D, and HCT-8 cells exposed to schedule D. Both cases showed consistent small Loewe synergy in three replicate experiments. There was no cell line which showed consistent Loewe synergy or Loewe antagonism across all incubation schedules. There were no striking differences in the results among the parent A2780/WT cell line, the PTX-resistant A2780/DX5B cell line, and the DDP-resistant A2780/CP3 cell line. There was no incubation schedule which showed consistent Loewe synergy or Loewe antagonism across all cell lines. The most promising schedule seemed to be schedule D (24 h PTX prior to 4 h DDP), which showed reproducible small Loewe synergy with the A121 and HCT-8 cell lines.

For a better characterization of the interaction surface, each experiment was explored through isobolographic examination. Isobols were plotted at 10%, 25%, 50%, 75% and 90% inhibition of cell growth. Figure 8A shows a representative example of Loewe antagonism, Fig. 8B shows an example of Loewe synergy and Fig. 9 shows three examples of Loewe additivity. The treatment of the A253 line with schedule A induced a clear Loewe antagonistic interaction all along the

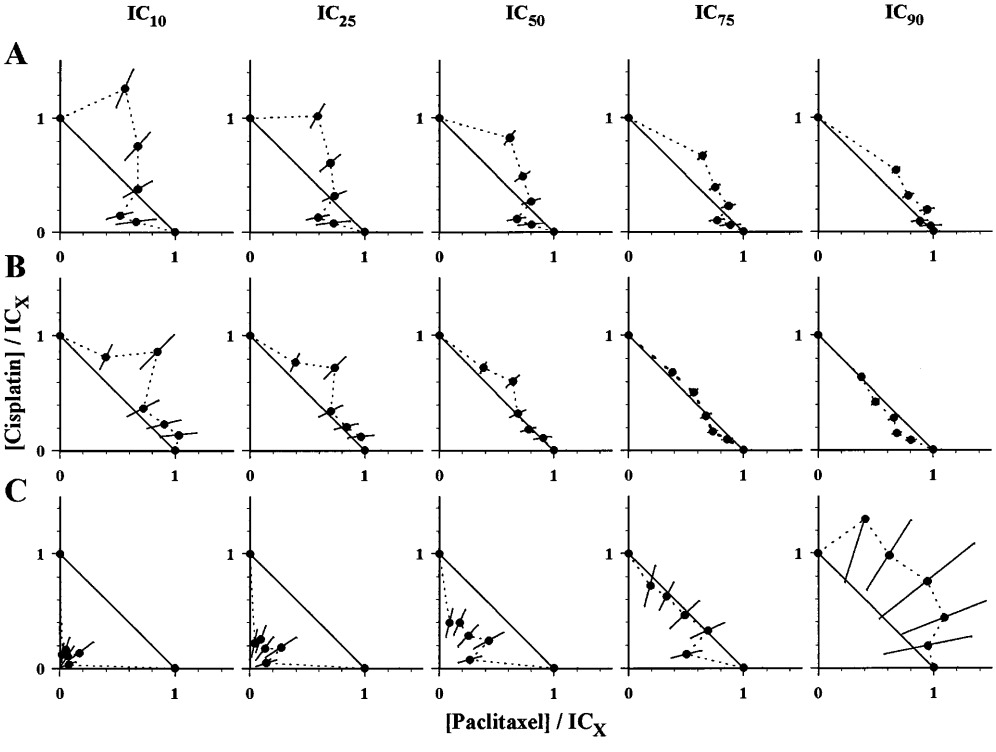

Fig. 9A–C Sets of normalized isobolograms for 10%, 25%, 50%, 75% and 90% inhibition of cell growth featuring Loewe additive combinations: **A** A2780/WT cells treated with schedule A ($\alpha = -0.00482 \pm 0.045$); **B** A253 cells treated with schedule A ($\alpha = 0.0724 \pm 0.050$); **C** A2780/WT cells treated with schedule F ($\alpha = 0.128 \pm 0.065$). The points are the observed IC_X values with accompanying 95% confidence intervals. The *straight diagonal line* is the theoretical Loewe additivity line

Table 2 Qualitative and quantitative characterization of the interactions PTX/PTX and DDP/DDP in the ovarian cell line A121, via the Universal Response Surface Approach. Cells were exposed to the combination with schedules A, D and E, in relation to the three schedules investigated and the two combinations. The results are presented as qualification of the interaction, e.g. Loewe additivity (*ADD*), Loewe synergy (*SYN*) or Loewe antagonism (*ANT*), followed by the estimate ± standard error of the interaction parameter α

	A	*D*	*E*
PTX/PTX	ADD 0.00495 ± 0.054	SYN 0.106 ± 0.040 SYN 0.813 ± 0.23	SYN 0.677 ± 0.24 SYN 0.951 ± 0.24
DDP/DDP	SYN 0.152 ± 0.049	SYN 0.134 ± 0.033 ADD 0.00655 ± 0.016	SYN 4.91 ± 1.1 ANT −0.0889 ± 0.0065

concentration-effect surface (Fig. 8A). This Loewe antagonism was confirmed with the URSA analysis ($\alpha = -0.0273 \pm 0.0056$). For A121 cells treated with schedule D ($\alpha = 1.40 \pm 0.23$), the combination yielded unambiguous Loewe synergistic isobols only for the higher effect levels (Fig. 8B), whereas at 10%, 25% and 50% of cell growth inhibition the combination induced a complex interaction surface with local Loewe antagonism changing to Loewe additivity or local Loewe synergy. The three examples of overall Loewe additivity shown in Fig. 9 include: A2780/WT, schedule A ($\alpha = -0.00482 \pm 0.045$, Fig. 9A); A253, schedule A ($\alpha = 0.0724 \pm 0.050$, Fig. 9B); A2780/WT, schedule F ($\alpha = 0.128 \pm 0.065$, Fig. 9C). The isobols seldom coincided with the theoretical Loewe additivity line. They had complex combined-action surfaces with regions of local Loewe antagonism and local Loewe synergy. Typical patterns of isobolographic behavior were described: (a) S-shape curve, implying local Loewe antagonism for DDP in excess associated with a Loewe additive or a Loewe synergistic component when its proportion in the mixture decreased (Fig. 9A); (b) reversed S-shape curve with local Loewe antagonism for PTX in excess associated with a Loewe additive or a Loewe synergistic component when its proportion dropped; (c) pure Loewe synergistic isobol moving to the Loewe antagonistic domain at high effect levels (Fig. 9C); (d) Loewe antagonistic curve collapsing toward the Loewe additivity line or even the Loewe synergistic region (Fig. 8A,B); and (e) near perfect Loewe additivity line (Fig. 8B, IC_{75} and IC_{90} levels). No obvious relationship between patterns of isobols, drugs, cell lines or conditions of exposure to the combinations could be drawn, as replicate experiments did not consistently induce similar isobols.

To serve as a negative control for Loewe antagonism or synergy, ten experiments were performed to investigate the effect on the ovarian cell line A121 of either PTX or DDP combined with itself. Only schedules A, D and E were investigated. Results of the data analysis are summarized in Table 2. The slight Loewe synergy ($\alpha = 0.152 \pm 0.049$) observed for DDP combined with itself for 96 h should, in principle, result only from dilution errors. The similar sham experiment performed with PTX yielded a true Loewe additive interaction, $\alpha = 0.00495 \pm 0.054$. In contrast, the sequential combination of PTX with itself (schedules D and E) was Loewe synergistic (α ranged from 0.106 to 0.951), possibly implying that the pretreatment of the cells with PTX induced cellular damage which could in turn have promoted the action of the subsequent administration of the drug. The sequential combination of DDP with itself (schedules D and E) yielded inconsistent results.

Discussion

We considered how PTX and DDP might act together at the cellular level. Studies conducted in vitro have demonstrated that PTX has no effect on DDP uptake, on the permeability of the plasma membrane for DDP or on intracellular glutathione or metallothionein levels [20, 30, 39]. Also, PTX pretreatment results in no increase in DDP-induced DNA interstrand and DNA-protein crosslinks [39]. PTX-mediated cell-cycle perturbation has been shown to occur, but only at drug concentrations well above those required for synergy with DDP [20]. Furthermore, DDP action is commonly considered to be independent of cell-cycle distribution [35]. DDP can possibly interfere with the cytochrome P450-dependent metabolism of PTX, since platinum compounds have been shown to modulate the activities of cytochrome P450 mixed-function oxidases [24].

In vitro studies of the combination PTX + DDP from other laboratories have yielded conflicting results, as shown in Table 3. For simultaneous exposure to the two drugs, synergy is seldom reported [2, 44]. The combination has been described as either additive [3, 9, 12, 22, 39, 46] or antagonistic [22, 23, 45]. When cells are treated with PTX prior to DDP, the interaction is either synergistic [20, 30, 39, 45], additive [9, 22, 26, 30, 45] or even antagonistic [9, 23]. Finally, when cells have been exposed to DDP prior to PTX, synergy has never been found. The combination is additive [9, 22, 23, 26, 30, 39] or antagonistic [9, 22, 26, 45]. The differences reported above for in vitro studies of the combination PTX + DDP may arise from (a) a large diversity of experimental settings, e.g. schedules investigated and

Table 3 Current status of the literature data for the combination PTX + DDP. The table entries include the reference number, the experimental settings and the results (*SYN* synergy, *ADD* additivity, *ANT* antagonism) of the two-drug interaction

Reference	Cell line	PTX + DDP exposure	Results
2	833 K (WT & 64CP10)	PTX + DDP 96 h	ADD-SYN
3	B16F10	PTX + DDP	ADD
12	H69 MCF-7	PTX + DDP 1 h	ADD
	OCI-MY7	PTX + DDP 3 h	ADD
		PTX + DDP 24 h	ADD
20	2008 (WT & C13)	DDP 1 h prior PTX 20 h	ANT
		PTX 19 h prior PTX + DDP 1 h	SYN
22	A549 MCF-7	PTX + DDP 24 h	ADD-ANT
	PA1 WiDr	PTX 24 h prior DDP 24 h	ADD
		DDP 24 h prior PTX 24 h	ADD-ANT
23	Ovarian specimen	PTX + DDP 120 h	ANT
		DDP prior PTX	ADD
		PTX prior DDP	ANT
26	A549 MCF-7	DDP 1 h prior PTX 24 h	ADD-ANT
		PTX 24 h prior DDP 1 h	ADD
30	A2780 (WT & CP70)	PTX + DDP 1 h prior PTX 23 h	ADD
		DDP 1 h prior PTX 24 h	ADD
		PTX 24 h prior DDP 1 h	ADD-SYN
39	L1210	PTX + DDP 24 h	ADD
		DDP 30 min prior PTX 24 h	ADD
		PTX 24 h prior DDP 30 min	SYN
44	Ovarian specimen	PTX + DDP	SYN-ANT-ADD
45	HM2 HM51	PTX + DDP 2 h	ANT
		DDP 2 h prior PTX 2 h	ANT
		PTX 2 h prior DDP 2 h	ADD-SYN
46	NSCL	PTX + DDP 96 h	ADD

duration of exposure, cell lines, end-points of measurement; (b) differences in the definition of the concept of additivity, e.g. Bliss independence, Loewe additivity; and (c) the subsequent variety in the methods of assessment of the nature and the intensity of the drug interaction [15], e.g. median effect analysis, isobologram by hand.

Our results showed that the combination PTX + DDP was overall Loewe additive for all cell lines and schedules. Similar results were obtained for wildtype and resistant A2780 cells and little schedule modulation was observed. Only for schedule D (24 h PTX prior to 4 h DDP), for cell lines A121 and HCT-8, was a departure from Loewe additivity reproducible. For these six experiments, in vitro Loewe synergy was very small (α ranging from 0.526 to 1.40). The isobolographic analysis showed a pure Loewe synergism only at high response levels, IC_{75} and IC_{90}. For 50% growth inhibition and below, the combination was either slightly Loewe antagonistic or Loewe additive. Therefore, in vitro Loewe synergy was rare, small and only reproducible in two out of seven cell lines, for one out of seven schedules. Interestingly, a small but reproducible intensity of Loewe synergy was obtained with the sham-sequenced combination PTX + PTX, which confirms the questionable importance of the Loewe synergy sporadically observed between PTX and DDP.

Surprisingly, for the 43 experiments which showed Loewe additivity, the isobol analysis rarely led to the straight line as expected from the Loewe additivity assumption, but rather led to highly complex combined-effect surfaces. It was critical to examine a large number of experimental design points to optimize the characterization of such complex surfaces. Several patterns of isobols were observed as mentioned above. Replicate experiments of a same drug exposure schedule in a same cell line did not systematically yield the same shapes of isobols. For instance, Fig. 8A,B shows two replicates of the growth inhibition induced by the treatment of the head and neck cells A253 with schedule A. As no consistent pattern of isobols was found either for a particular schedule, or for a particular cell line, the clinical implications of these in vitro findings remain unclear. Furthermore, these in vitro results underscore the caution that investigators should take in interpreting any interesting but unreproduced isobol. Objective quantitative assessments of combined-action of replicated experiments are essential.

In contrast to the combination PTX + DDP, other combinations of agents, such as AraC + DDP [14], trimetrexate + lometrexol [8] or trimetrexate + various polyglutamylatable antifolates [6], have been shown by our group with similar experimental methods [6] and the same modeling methodology [6, 8, 14] to yield highly reproducible Loewe synergy. The method is able to detect small to extremely large levels of Loewe synergy. Therefore, the lack of observed Loewe synergy found for

PTX + DDP is unlikely to be a consequence of problems with our experimental or statistical methodology.

Single-drug therapy seldom cures cancer and combinations are necessary to produce good clinical efficacy [5]. Theoretically, the achievement of higher total dose provides a maximal cell kill with respect to the toxicity. If the combined agents have a nonoverlapping pattern of organ toxicity, full dosage of each agent can be used and the effectiveness of each drug is fully maintained. With neutropenia and nephrotoxicity, respectively, as dose-limiting toxicities, PTX and DDP fulfill this first requirement, although clinically they are used at reduced dosages when combined [13]. (Note that owing to a 33% decrease in PTX total body clearance, and therefore an enhanced myelosuppression if DDP precedes PTX, PTX is clinically given first as a 3-h or 24-h infusion followed by DDP [38].) A second rationale for combination therapy is that initial resistance to a given single drug is frequent; combining agents with different mechanisms of action provides a broader coverage of an intrinsically heterogeneous tumor cell population. The combination PTX + DDP fulfills this second rationale. A third rationale is that the combination would reduce the probability of the development of new resistance resulting from drug-induced mutation or selection of initially resistant cells. The combination PTX + DDP again qualifies. Finally, the combined agents may biochemically interact at the cellular level. This last point can be studied in in vitro experiments such as those presented in this report. The apparent decrease caused by anticancer agents in the endpoint measured by in vitro tumor cell growth inhibition assays is the combined result of cell death, cytostasis and cell growth slowdown. In order to tease out the contributions of these three components of apparent growth inhibition, image analysis-based methods are currently under development in our laboratory and will provide insights on drug effect at the individual colony level [41] and at the individual cell level [17]. However, in vitro to in vivo extrapolation should always be cautiously considered, since cancer cells grown as a monolayer lack interactions with surrounding tissue and blood which could alter the cellular response to a particular drug or combination.

As the in vitro Loewe synergy reported in the present study was small and poorly reproducible among several cell lines treated with several clinically inspired schedules, it is unlikely that the clinical efficacy of this combination arises from an interaction at the cellular level. It appears more likely that the therapeutic efficacy of the combination PTX + DDP results from the achievement of a high dosage of each agent arising from a nonoverlapping spectrum of organ toxicity and results from a wide coverage of an heterogeneous tumor cell population.

Acknowledgements The authors thank Elva Winslow and Piao Ji for technical assistance and John C. Parsons for computer expertise. We also thank Hélène Faessel, Udo Vanhoefer and Mark F. Brady for helpful discussions.

References

1. Ajani JA, Ilson DH, Kelsen DP (1995) The activity of paclitaxel in gastrointestinal tumors. Semin Oncol 22 [Suppl 12]: 46
2. Chou TC, Motzer RJ, Tong Y, Bosl GJ (1994) Computerized quantitation of synergism and antagonism of taxol, topotecan, and cisplatin against human teratocarcinoma cell growth: a rational approach to clinical protocol design. J Natl Cancer Inst 86: 1517
3. Chu QD, Shrayer DP, Wanebo HJ (1995) Biophasic effect of cisplatin and taxol on B16 F10 melanoma. Proc Am Assoc Cancer Res 36: A2218
4. Crickard K, Niedbala MJ, Crickard U, Yoonessi M, Sandberg AA, Okuyama K, Bernacki RJ, Satchidanand SK (1989) Characterization of human ovarian and endometrial carcinoma cell lines established on extracellular matrix. Gynecol Oncol 32: 163
5. DeVita VT (1993) Principles of chemotherapy. In: DeVita VT Jr, Hellman S, Rosenberg SA (eds) Cancer: principles and practices of oncology, 4th edn. JB Lippincott, Philadelphia, p 276
6. Faessel H, Slocum HK, Jackson RC, Boritzki T, Rustum YM, Greco WR (1996) Super in vitro synergy between trimetrexate and the polyglutamylatable antifolates AG2034, AG2032, AG2009 and Tomudex against human HCT-8 colon cells. Proc Am Assoc Cancer Res 37: A2629
7. Forastiere AA (1994) Current and future trials of taxol (paclitaxel) in head and neck cancer. Ann Oncol 5: S51
8. Gaumont Y, Kisliuk RL, Parsons JC, Greco WR (1992) Quantitation of folic acid enhancement of antifolate synergism. Cancer Res 52: 2228
9. Gercel-Taylor C, Taylor D, Owens K (1994) Effect of sequencing with taxol on cisplatin sensitivity of ovarian cancer cell lines. Proc Am Assoc Cancer Res 35: A1959
10. Gessner PK (1974) The isobolographic method applied to drug interactions. In: Morselli PL, Garattini S, Cohen SN (eds) Drug interactions. Raven Press, New York, p 349
11. Giard DJ, Aaronson SA, Todaro GJ, Kersey JH, Dosik H, Parks WP (1973) In vitro cultivation of human tumors: establishment of cell lines derived from a series of solid tumors. J Natl Cancer Inst 51: 1417
12. Glück S, Sharan N, Chadderton T, Dietz G, Bewick M, Köster W, Lutynski A, Gallant G (1994) In vitro combination of paclitaxel (Taxol®, TXL) with 5 different cytotoxic drugs: effect on three different cell lines. Proc Am Assoc Cancer Res 35: A1992
13. Greco FA (1996) Urogenital and gynecologic cancer. In: Greco FA (ed) Handbook of commonly used chemotherapy regimens. A quick reference guide to more than 100 current cytotoxic therapies. Precept Press, Chicago, p 137
14. Greco WR, Park HS, Rustum YM (1990) An application of a new approach for the quantitation of drug synergism to the combination of cis-diamminedichloroplatinum and 1-β-D-arabinofuranosylcytosine. Cancer Res 50: 5318
15. Greco WR, Bravo G, Parsons JC (1995) The search for synergy: a critical review from a response surface perspective. Pharmacol Rev 47: 331
16. Greene RF, Chatterji DC, Hiranaka PK, Galleli JF (1979) Stability of cisplatin in aqueous solution. Am J Hosp Pharm 36: 38
17. Grunwald J (1987) Time-lapse video microscopic analysis of cell proliferation, motility and morphology: applications for cytopathology and pharmacology. Biotechniques 5: 680
18. Hortobagyi GN (1995) Management of breast cancer: status and future trends. Semin Oncol 22: 101
19. Jamali MAA, Yin MB, Mazzoni A, Bankusli I, Rustum YM (1989) Relationship between cytotoxicity, drug accumulation, DNA damage and repair of human ovarian cancer cells treated with doxorubicin: modulation by the tiapamil analog RO11-2933. Cancer Chemother Pharmacol 25: 77

20. Jekunen AP, Christen RD, Shalinsky DR, Howell SB (1994) Synergistic interaction between cisplatin and taxol in human ovarian carcinoma cells in vitro. Br J Cancer 69: 299
21. Johnson DH (1995) Phase III trial (E5592) comparing cisplatin plus etoposide with cisplatin plus paclitaxel at two dose levels for treatment of advanced non-small-cell lung cancer. Eastern Cooperative Oncology group. Monogr Natl Cancer Inst 19: 61
22. Kano Y, Akutsu M, Tsunoda S, Suzuki K, Yazawa Y (1996) In vitro schedule-dependent interaction between paclitaxel and cisplatin in human carcinoma cell lines. Cancer Chemother Pharmacol 37: 525
23. Kern DH, Morgan CR (1993) Apparent in vitro antagonism between cisplatin and taxol. Proc Am Assoc Cancer Res 34: A1788
24. LeBlanc GA, Sundseth SS, Weber GF, Waxman DJ (1992) Platinum anticancer drugs modulate P-450 mRNA levels and differentially alter hepatic drug and steroid hormone metabolism in male and female rats. Cancer Res 52: 540
25. Levasseur L, Faessel H, Slocum HK, Greco WR (1995) Precision and pattern in 96-well plate cell growth experiments. Proc Biopharm Sect Am Stat Assoc: 227
26. Liebmann JE, Fisher J, Teague D, Cook JA (1994) Sequence-dependence of paclitaxel (Taxol®) combined with cisplatin or alkylators in human cancer cells. Oncol Res 6: 25
27. Lopes NM, Adams EG, Pitts TW, Bhuyan BK (1993) Cell cycle kinetics and cell cycle effects of taxol on human and hamster ovarian cell lines. Cancer Chemother Pharmacol 32: 235
28. Masuda H, Ozols RF, Lai GM, Fojo A, Rothenberg M, Hamilton TC (1988) Increased DNA repair as a mechanism of acquired resistance to cisdiamminedichloroplatinum(II) in human ovarian cancer cell lines. Cancer Res 48: 5713
29. McGuire WP, Hoskins WJ, Brady MF, Kucera PR, Partridge DE, Look KY, Clarke-Pearson DL, Davidson M (1996) Cyclophosphamide and cisplatin compared with paclitaxel and cisplatin in patients with stage III and stage IV ovarian cancer. N Engl J Med 334: 1
30. Parker RJ, Dabholkar MD, Lee KB, Bostick-Bruton F, Reed E (1993) Taxol effect on cisplatin sensitivity and cisplatin cellular accumulation in human ovarian cancer cells. Monogr Natl Cancer Inst 15: 83
31. Parker RJ, Lee KB, Dabholkar M, Bostick-Bruton F, Simms M, Reed E (1993) Influence of taxol: cisplatin sequencing on cisplatin-DNA adduct repair in human ovarian cancer cells. Proc Am Assoc Cancer Res 34: A2122
32. Peyrot V, Briand C, Crevat A, Braguer D, Chauvet-Monges AM, Sari JC (1983) Action of hydrolyzed cisplatin and some analogs on microtubule protein polymerization in vitro. Cancer Treat Rep 67: 641
33. Rangan SRS (1972) A new human cell line (FaDu) from a hypopharyngeal carcinoma. Cancer 29: 117
34. Reed E, Kohn EC, Sarosy G, Dabholkar M, Davis P, Jacob J, Maher M (1995) Paclitaxel, cisplatin, and cyclophosphamide in human ovarian cancer: molecular rationale and early clinical results. Semin Oncol 22: 90
35. Reed E, Dabholkar M, Chabner BA (1996) Platinum analogues. In: Chabner BA, Longo DL (eds) Cancer chemotherapy and biotherapy: principles and practice. Lippincott-Raven, Philadelphia New York, p 357
36. Rogan AM, Hamilton TC, Young RC, Klecker RW, Ozols RF (1984) Reversal of adriamycine resistance by verapamil in human ovarian cancer. Science 224: 994
37. Rowinsky EK, Cazenave LA, Donehower RC (1990) Taxol: a novel investigational antimicrotubule agent. J Natl Cancer Inst 82: 1247
38. Rowinsky EK, Gilbert M, McGuire WP, Noe DA, Grochow LB, Forastiere AA, Ettinger DS, Lubejko BG, Clark B, Sartorius SE, Cornblath DR, Hendricks CB, Donehower RC (1991) Sequences of taxol and cisplatin: a phase I and pharmacologic study. J Clin Oncol 9: 1692
39. Rowinsky EK, Citardi MJ, Noe DA, Donehower RC (1993) Sequence-dependent cytotoxic effects due to the combinations of cisplatin and antimicrotubule agents taxol and vincristine. J Cancer Res Clin Oncol 119: 727
40. Skehan P, Storeng R, Scudiero D, Monks A, McMahon J, Vistica D, Warren JT, Bokesch H, Kenney S, Boyd MR (1990) New colorimetric cytotoxicity assay for anticancer-drug screening. J Natl Cancer Inst 82: 1107
41. Slocum HK, Malmberg M, Greco WR, Parsons JC, Rustum YM (1990) The determination of growth rates of individual colonies in agarose using high resolution automated image analysis. Cytometry 11: 793
42. Thigpen T, Vance R, Puneky L, Khansur T (1994) Chemotherapy in advanced ovarian carcinoma: current standards of care based on randomized trials. Gynecol Oncol 55: S97
43. Thigpen T, Vance RB, Khansur T (1995) The platinum compounds and paclitaxel in the management of carcinomas of the endometrium and uterine cervix. Semin Oncol 22 [Suppl 12]: 67
44. Untch M, Sevin BU, Perras JP, Angioli R, Untch A, Hightower RD, Koechli O, Averette HE (1994) Evaluation of paclitaxel (Taxol), cisplatin, and the combination paclitaxel-cisplatin in ovarian cancer in vitro with the ATP cell viability assay. Gynecol Oncol 53: 44
45. Vanhoefer U, Harstrick A, Wilke H, Schleucher N, Walles H, Schröder J, Seeber S (1995) Schedule-dependent antagonism of paclitaxel and cisplatin in human gastric and ovarian carcinoma cell lines in vitro. Eur J Cancer 31A: 92
46. Viallet J, Boucher L, Gallant G (1994) In vitro interactions between paclitaxel (TAX) and other agents in human non small cell lung cancer (NSCLC) cell lines: antagonism with etoposide (VP-160) and doxorubicin (DOX). Proc Am Soc Clin Oncol 13: A1233